THE ASTROPHYSICAL JOURNAL, 469:138–146, 1996 September 20

ON THE ORIGIN OF THE SOUTHWEST Hα REGIONS OF THE SPIRAL GALAXY NGC 3367

J. A. GARCÍA-BARRETO, J. FRANCO, AND R. CARRILLO
Instituto de Astronomía, Universidad Nacional Autónoma de México, Apartado Postal 70-264, México D.F. 04510, México
Received 1995 October 16; accepted 1996 April 4

ABSTRACT

New narrow-band, continuum-free, Hα, and broadband *R* and *I* imaging data from the barred galaxy NGC 3367 are presented. Our Hα observations indicate that there is Hα almost all over the disk of the galaxy, and there are no particular signs of either nuclear or outer rings. Strong Hα emission is detected from the compact nucleus and from different sources in the disk. In particular, there are H II regions at the ends of the stellar bar and in the inner spiral arms. Also, and very strikingly, a string of Hα emission sources spanning almost 180°, from southeast to northwest, is observed in the southwest region of the galaxy, at an almost constant radius from the center. The string is located outside the stellar bar and does not belong to any particular spiral arm. There are several possible interpretations regarding the origin of these Hα knots (i.e., due to an outer Lindblad resonance ring, to the interaction of NGC 3367 with a hot intergalactic medium, or to a direct impact with a neighbor), but we favor the possibility that the string is due to an off-center impact by an intruder. This scenario can also explain the emission from the compact nucleus and is consistent with the expected lifetimes of the Hα knots and the kinematic timescales for an induced ring by an intruder. The string of Hα sources is probably evidence of having cloud overlap, which has triggered new massive star formation.

Subject headings: galaxies: individual (NGC 3367) — galaxies: photometry — galaxies: spiral — galaxies: structure

1. INTRODUCTION

NGC 3367 is an almost face-on SBc(s) barred spiral galaxy, and its disk is inclined with respect to the line of sight at an angle of $i \sim 6°$ (Grösbol 1985). The stellar bar has an angular diameter of $\sim 32''$, and it is oriented at a position angle of about 65°. The centroid of the atomic hydrogen emission corresponds to a radial velocity of $v \simeq 3040$ km s^{-1}, and the 21 cm line has an FWHM $\simeq 260$ km s^{-1} (Huchtmeier & Seiradakis 1985; Staveley-Smith & Davies 1988; Mirabel & Sanders 1988). NGC 3367 belongs, together with NGC 3419, to the group 32−4+4 of Tully (1988), with a distance of 43.6 Mpc (i.e., using $H_0 = 75$ km s^{-1} Mpc^{-1} and assuming that the Milky Way is moving toward the Virgo Cluster at 300 km s^{-1}) and lies behind the Leo Spur group of galaxies. At that distance, an angular scale of 1″ corresponds to some 210 pc.

There are several interesting features about this barred galaxy. Its optical morphology is peculiar, the light is distributed asymmetrically (see, for example, Sandage 1962) and its southwest structure resembles a "bow shock." Optical spectroscopy of the central regions by Véron-Cetty & Véron (1986) shows a broad Hα line with FWHM ≤ 600 km s^{-1}, and O III and N II lines suggestive of a Seyfert-like nucleus. The X-ray emission in the direction of the NGC 3367 region has been studied with the *Einstein Observatory* by Gioia et al. (1990), Stocke et al. (1991) and Fabbiano, Kim, & Trinchieri (1992). There is a strong X-ray emission peak coincidental with the optical galaxy, but its centroid is displaced from the optical compact nucleus by some 21″ in the southwest direction (Stocke et al. 1991). NGC 3367 is also a relatively strong far-infrared (FIR) emitter, and its FIR luminosity, obtained by *IRAS*, is of about $L_{\rm FIR} \sim 2 \times 10^{10}\, L_\odot$ (Soifer et al. 1989). Compared with other barred galaxies, it has a relatively high dust temperature of $T_D \simeq 35$ K (García-Barreto et al. 1993).

In this paper we present new *R*, *I*, and Hα imaging observations of NGC 3367. The Hα image shows several distinctive interesting regions: emission from the compact nucleus, from the spiral arms, from the northeast end of the stellar bar, lack of emission from the stellar bar region, and emission from a set of bright sources at a constant distance from the nucleus (from the southeast to the northwest, passing through the southwest edge of the galaxy). The presence of gas in the compact nucleus is most likely a result of accretion from the outer regions, either by the dynamics imposed by a nonaxisymmetric gravitational field (Phinney 1994) or by an interaction with an intruder and/or companion (Toomre 1978). The semicircular string of H II regions, on the other hand, could be the result of a series of different reasons, but we favor the possibility of an interaction with an intruder. Both features, nuclear emission and the string of H II regions in the southwest, could then be explained naturally by a single mechanism. Section 2 presents the observations and results, § 3 discusses several possible mechanisms for the origin of the string of Hα knots and, finally, § 4 gives the conclusions.

2. OPTICAL OBSERVATIONS: THE DISTRIBUTION OF Hα EMISSION

We have carried on optical observations at the Observatorio Astronómico Nacional in San Pedro Mártir, Baja California, México, usng the 2.12 m telescope f/7.5, equipped with a CCD detector of 1024 × 1024 pixels together with the broadband Johnson filters *R* and *I*, and the narrow-band filters centered at the wavelength of Hα for imaging. The detector scale gives a spatial resolution of 0.″25 per pixel in the imaging mode, giving a field of view of 4.′25 × 4.′25. Details of the observations are summarized in Table 1.

The images were bias subtracted and then flat-fielded by using an average of three similar 1 s exposures of blank fields taken at twilight. The images were then flat-fielded

TABLE 1

IMAGING OBSERVATIONS OF THE BARRED GALAXY NGC 3367

Filter	Date	Instrument	λ_c (Å)	$\Delta\lambda$ (Å)
R.....	1993 Dec 15	CCD 1024 × 1024	6340	400
I	1993 Dec 15	CCD 1024 × 1024	8040	1660
$H\alpha_{cont}$.....	1993 Dec 15	CCD 1024 × 1024	6459	101
Hα	1993 Dec 15	CCD 1024 × 1024	6607	89

using different flats for each filter. Each flat consisted of a 60 s exposure for the narrow filters, and a 30 s exposure for the broadband filters. Two images were taken with the broadband filters R and I, each exposure 90 s long. Two more images, each exposure 300 s long, were taken also with narrow-band filters centered at $\lambda \simeq 6459$ Å with $\Delta\lambda \simeq 101$ Å, for the continuum, and at $\lambda \simeq 6607$ Å with $\Delta\lambda \simeq 89$ Å for the redshifted Hα plus continuum. The data reduction was performed with the IRAF software package developed at NOAO. All images were calibrated and edited for cosmic rays. The final Hα images were obtained by subtracting the continuum. In order to do this, we selected the line + continuum and continuum images each of 300 s integration time each observed after the other with similar sky conditions. Positions of field stars from both images were determined in order to assure their alignment. The image scale was 1:1 for the subtraction. After the subtraction, the field stars disappeared completely from the final Hα emission image. The seeing in 1993 December was about 1″–1.″5 with clear sky. The Hα image was amplitude calibrated using as a flux calibrator the star Feige 24 $\alpha(1950) = 2^h32^m.5$, $\delta(1950) = +3°31'$ with a flux at Hα as $F_\alpha \simeq 1.485 \times 10^{-10}$ ergs s^{-1} cm^{-2} (Oke 1974; Oke & Schild 1970). Note that our Hα image also includes the N [II] emission lines, since our filter had an FWHM bandwidth of 89 Å.

Figures 1*a* and 1*b* (Plate 2) show the images of NGC 3367 in the broadband R and I filters, Figure 2 (Plate 3) shows the $R+I$ image, and Figure 3 (Plate 4) shows the $R-I$ image. Figure 4 (Plate 5) shows the Hα image on which we have labeled, from 1 to 9, the brightest knots in the southwest half-ring structure. Both the R and I images show an enhancement of the surface brightness at the southwest regions of the galaxy. One sees the bright and smooth stellar bar at P.A. $\simeq 65°$, and its total length is about 32″, which corresponds to a diameter of about 6.7 kpc. The stellar bar radius is about $\frac{1}{3}$ of the bright optical disk of the galaxy. There are two spiral arms apparently originating from the northeast end of the stellar bar. One of them terminates at the northwest side of the galaxy, making an angle of more than 30° with the semicircle of Hα emission knots (see below). The other spiral arm curves inward passing by the southwest end of the bar, ending parallel to the semicircle of Hα emission knots at the south. A smooth extended emission comes from about all the disk. A pair of structures is seen at the southeast side of the stellar bar. Both are bright in R and I images, with some bright knots seen also in the Hα image. The brightness of the eastern most structure ends abruptly. This is probably intrinsic, since there is no indication of redder emission contributing to extinction in that region as seen in the $R-I$ image (Fig. 3). A double-arm structure on one side of a stellar bar similar to the structure seen at the east side of NGC 3367 can be seen in the barred spiral galaxy NGC 2525 at its southeast side (García-Barreto et al. 1996).

The strongest Hα emission comes from the compact nucleus. The disk displays a series of knots delineating the spiral arms seen in the R and I images. Several H II regions are seen at the northeast end of the stellar bar and at the southeast side of the bar. There is also a southwest Hα structure that appears as a half-ring. Each of these Hα knots is about 2″ in diameter, or 420 pc, and their relative intensities indicate that the number of stars in the exciting clusters (a few hundred OB stars per region) is similar to those derived for star-forming regions in other barred galaxies, like NGC 1326 or NGC 4314 (García-Barreto et al. 1991a, 1991b). There is no Hα emission detected from the bar to a limit of about less than 1/500 of the flux of the compact nucleus, indicating that the star formation activity in the bar is null compared with the rest of the galaxy.

Two Hα emission features that deserve an extended discussion in this paper are the compact nucleus and the southwest collection of knots forming the "half-ring," extending from the southeast to the northwest at a nearly constant galactocentric distance of ~9–10 kpc.

2.1. Hα *Emission from the Nucleus (Inner 5″)*

The FWHM of the Hα emission from the compact nucleus is ~2.″2, or about 450 pc, and the FWZI extends to 6″. Except for its large strength, this nuclear emission does not seem to be unusual for this type of galaxy. Even when we cannot rule out completely the possible existence of a circumnuclear ring at the inner Lindblad resonances (ILRs), with an average radius of about 200 pc and a similar width, the present data are consistent with the absence of such a ring. Plots of the Hα cross section at the galaxy center do not show any evidence of the expected two-peak maximum. Instead, they show a simple line that can be fitted by a single Gaussian. This is in agreement with the observation of other barred galaxies, which show no ILR circumnuclear rings but instead do show IR and Hα emission from the nucleus (Telesco, Dressel, & Wolstencroft 1993, García-Barreto et al. 1996).

2.2. *Knots of* Hα *Emission from the External Regions*

Hα emission was detected from several places in the disk; at the northeast end of the bar, from the H II regions to the southeast of the bar, from H II regions at the spiral arms (with an FWHM below 2″), and from a series of sources arranged as pearls in a necklace in the outer regions of the galaxy (see Fig. 4). The total Hα flux within a radius of about 47″ (including the emission from the compact nucleus) is $F(H\alpha) \simeq 3.4 \times 10^{-12}$ ergs s^{-1} cm^{-2}. Figure 5 (Plate 6) shows the Hα emission contours superimposed on the $R+I$ continuum image. One can see the contours of the southwest knots (labeled 2, 3, and 4) and also those from the spiral arm north of them. The separation between the southwest knots and the spiral arm is clear.

The distribution of bright knots in the southwest outer region is highly symmetrical. It starts at the southeast and goes around the galaxy all the way to the northwest, covering a semicircle of about 180°, at an average radius of 42″ (or 9 kpc) from the center. There is no emission at the same radius in the northwest-southeast regions of the galaxy. Table 2 lists only the relative positions and Hα fluxes of the southwest brightest knots. The average FWHM of each region is about 2″, or about 420 pc. The most likely origin for the emission from these knots is star formation with massive OB stars. The required number of OB stars is

TABLE 2

RELATIVE POSITIONS AND INTENSITIES ONLY OF THE SOUTHWEST Hα KNOTS IN NGC 3367

Knot	ΔR.A. (arcsec)	ΔDecl. (arcsec)	FWHM (arcsec)	Distance (kpc)	Peak Intensity[a] (ergs s^{-1} cm^{-2})
1.....	+16.0	−38.0	2.1	8.8	12.0
2.....	+10.0	−41.0	2.1	9.0	4.8
3.....	−2.3	−43.0	2.1	9.1	4.4
4.....	−12.0	−40.0	1.9	8.8	8.2
5.....	−18.0	−36.0	Indefinite	8.5	3.0
6.....	−47.0	−9.0	Indefinite	10.0	2.3
7a	−48.0	−5.0	1.9	10.2	18.5
7b	−46.0	−4.0	2.12	10.1	14.8
8.....	−48.0	+4.0	2.6	10.2	4.3
9.....	−44.0	+27.0	2.9	10.9	5.7
Nucleus.....	0.0	0.0	2.0	0.0	238.0

NOTE.—Relative positions were taken relative to nucleus. Positions, relative strengths, and FWHM were taken from the routine SPLOT in IRAF. Distance from the compact nucleus is assuming NGC 3367 is at 43.6 Mpc.

[a] Flux of Hα in units of 10^{-15}.

similar to those inferred for H II regions in other barred spiral galaxies: several thousand OB stars per region.

The southwest string of emission comes from an extended radio continuum emission region. This radio region is weaker than the southwest strong radio continuum peak. Figure 6 shows a superposition of the radio contours on the Hα image. Notice that the radio continuum map seems to be also broader in the southwest region compared to the northeast. There are some weak Hα knots at the position of the northeast and southwest bright radio continuum sources straddling the nucleus. These two radio sources are aligned at a different P.A. than the optical bar.

The *R* image shows a spiral arm that originates at the northeast tip of the stellar bar and goes around all the way to the southwest. The Hα knots labeled 3, 4, and 5 in Figure 4 could be thought to belong to that arm, but they are not related. There is a declination difference of about 9″, 8″, and 11″, respectively, between the spiral arm in the *R* image and the Hα knots to the south. The *R* image shows an additional spiral arm that also originates at the northeast tip of the

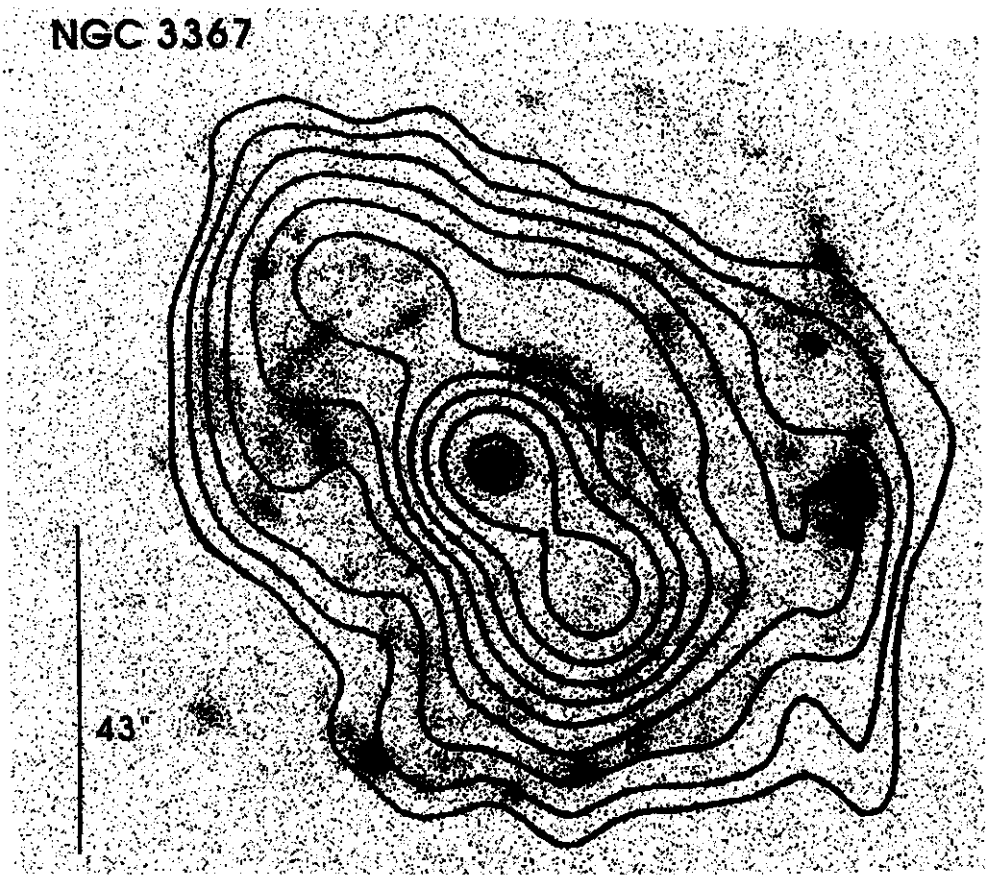

FIG. 6.—Radio continuum (20 cm) contours superimposed on the Hα image (gray scale). The radio continuum is taken from Condon et al. (1990), with a resolution of 15″.

stellar bar but goes around to the west side of the galaxy. This arm is located at the north of the previously described arm (see Fig. 1). Knots 6, 7a, 7b, 8, and 9 are easily observed in the *R* image, but their orientations are not parallel to the arm (ΔP.A. $\geq 40°$). There is evidence that suggests that the Hα knots in the southwest do not belong to any particular spiral arm. Notice that there is definitely no evidence of any red continuum or Hα emission from a similar distance at the northeast semicircle of the galaxy.

The distribution of Hα emission from the southwest edge of the galaxy is rather peculiar, and its morphology is similar to the one seen in broadband optical photographs (Sandage 1962). Neither image, blue, red, or narrow-line, shows evidence for the existence of a complete ring. In fact, the morphology of the southwest region of the galaxy has a sharp edge, shaped as a "bow shock." Although Hα is observed almost all over the disk, the semicircle indicates an enhancement of recent star formation at about a constant distance from the galaxy center: something triggered a coherent star formation activity at the outer edge of the galaxy. In the next section, we discuss several possible scenarios for its origin.

3. DISCUSSION

This section explores the possible origin of the Hα in the central region of the galaxy, as well as the southwest string of Hα sources. Regarding the central region, we describe its position as given by several authors. In the case of the southwest string, we explore the following scenarios: (*a*) the string is part of an outer Lindblad resonance ring, (*b*) the string is due to the interaction of NGC 3367 with intergalactic gas, as it travels into the southwest direction, and (*c*) the string is the result of a direct interaction. We favor the last possibility, that the string was formed by an off center impact with an external perturber. This mechanism and the action of the nonsymmetric gravitational potential from the bar could also drive a vigorous gas inflow to the compact nucleus in a relatively short timescale. Thus, three observational facts can be addressed with an impulsive perturbation in NGC 3367: the presence of gas at the compact nucleus, lack of any ionized gas from the stellar bar region, and the southwest string of Hα sources at a constant distance from the center.

3.1. *The Gas Content of NGC 3367*

Neutral hydrogen studies indicate that NGC 3367 is a gas-rich Sc galaxy. From the definition of "H I deficiency" given by Giovanelli, Chincarini, & Haynes (1981), H I Def $\simeq \langle \log (M_H/L_B) \rangle_{cs} - \log (M_H/L_B)$, and using the average value of their control sample for Sc galaxies and a total H I mass $M_{HI} = 6 \times 10^9\ M_\odot$ (for a distance of 43.6 Mpc; Giovanardi et al. 1983; Huchtmeier & Seiradakis 1985), we obtain H I Def $\simeq +0.52$. This H I deficiency value is within the values expected for "normal" disk galaxies, and one can conclude safely that NGC 3367 has not suffered any recent episode of gas removal.

With respect to the molecular phase, although there are no CO observations reported yet for NGC 3367, one can estimate the amount of molecular gas following the correlations found by Young et al. (1986) for bright far-infrared galaxies. From the far-infrared *IRAS* luminosity, the expected molecular gas content in NGC 3367 is $M_{H_2} \sim 5 \times 10^8\ M_\odot$, or about 10% of the atomic mass. Similarly, the estimated dust mass is $M_D \sim 10^6\ M_\odot$, which corresponds to a dust-to-gas mass ratio that is a factor of about 1/10 the Galactic value. The resulting total gas content is about $M_T \sim 7 \times 10^9\ M_\odot$, which is similar to the total gas content of other bright far-infrared galaxies (Young et al. 1986). The estimated star formation rate of O, B, and A stars can be obtained from the expression given by Scoville & Young (1983):

$$M_{OBA} \sim 7.7 \times 10^{-11} \left(\frac{L_{TOT}}{L_\odot}\right) M_\odot\ \mathrm{yr}^{-1} \simeq 5\ M_\odot\ \mathrm{yr}^{-1}\ ,$$

which is also similar to the rates derived for other bright infrared galaxies (see Table 4). Thus, both the estimated gas content and star formation rate are within the range of values expected for Sc galaxies.

3.2. *Position of the Nucleus*

In Table 3 we list the positions associated with the compact nucleus of NGC 3367 by several authors. Humason, Mayall, & Sandage (1956) observed the nucleus using the position given in the NGC catalog. *IRAS* observations give the position for the centroid of the galaxy. Condon et al. (1990) gives the exact position of the two brightest, but unresolved, radio continuum sources observed with the VLA at 20 cm. The position of the brightest radio continuum peak is offset from the *IRAS* centroid $+13''$ in R.A. and $-6''$ in declination. The X-ray emission centroid (Stocke et al. 1991) is offset from the VLA brightest radio continuum source by $-19''$ in R.A. and $-10''$ in declination. These offsets, however, are within the error bars and cannot be really regarded as relevant. Figure 6 shows the superposition of our Hα image and the radio continuum emission contours at 20 cm from Condon et al. (1990). This superposition was done assuming that the brightest radio continuum source coincides with the central Hα emission source. This assumption seems reasonable, since other Hα sources in the west side, like those labeled 6 and 7, coincide with the radio continuum emission.

3.3. *Gas in the Central Region of NGC 3367*

Spectroscopic studies by Véron-Cetty & Véron (1986) show relatively broad Hα and [N II] emission lines for NGC 3367, with FWHM velocities of up to 600 km s^{-1}, which would suggest a Seyfert-like spectrum. The Hβ intensities, on the other hand, are about twice the [O III] λ5007 intensities, and it would be difficult to call it a Seyfert 2 galaxy (for which [O III] $\gg$ Hβ) or a low-ionization nuclear

TABLE 3

POSITIONS OF THE NUCLEUS OF NGC 3367

R.A. (1950.0)[a]	Decl. (1950.0)[b]	Method	Reference
10 44.0	+14 01	Optical	1
10 43 55.8 ± 2	+14 00 50 ± 4	Optical	2
10 43 55.40 ± 4	+14 00 58 ± 4	Optical	3
10 43 56.0	+14 00 48	Optical	4
10 43 54.7	+14 00 58	Far-IR	5
10 43 55.6	+14 00 52	Radio (20 cm)	6
10 43 54.7	+14 00 41.1	X-ray	7

[a] In units of hours, minutes, and seconds.

[b] In units of degrees, arcminutes, and arcseconds.

REFERENCES.—(1) Humason, Mayall, & Sandage 1956; (2) Gallouet & Heidmann 1971; (3) Dressel & Condon 1976; (4) Sandage & Tammann 1981; (5) *IRAS* Point Source Catalog 1988; (6) Condon et al. 1990; (7) Gioia et al. 1990.

emission-line region (LINER) (for which [O I] ≥ 0.3Hα). Ho, Filippenko, & Sargent (1995) also report unusually broad lines (FWHM ~ 490 km s^{-1} for Hβ) and intensity ratios of emission lines suggesting a mixture of H II regions and a LINER, with a possible presence of W-R stars. Thus, NGC 3367 has a bright compact nucleus with ionized gas but does not show clear signs of active galactic nucleus (AGN) activity.

NGC 3367 is a relatively strong VLA radio continuum emitter, with 99 mJy total flux at 20 cm (Condon et al. 1990). The radio continuum emission comes from almost all around the galaxy, in addition to three strong peaks of emission: a central emission region plus two others straddling it at opposite sides, at a distance of about 22″ in the northeast-southwest direction but at about 20° different P.A. than the stellar bar ($\simeq 45°$ vs. $\simeq 65°$ for the stellar bar). As stated before, the position of the central radio peak is offset with respect to the infrared position given by *IRAS*.

The emission at the center suggests that some fresh gas has been accreted recently into the nucleus, and it is powered presently by photoionization from young stellar clusters. With respect to the source of fresh gas, there are several mechanisms that could drive the gas all the way in: angular momentum transfer as the gas crosses the bar region (i.e., due to the dynamics imposed by a nonaxisymmetric gravitational potential; Lynden-Bell & Kalnajs 1972, Simkin, Su, & Schwarz 1980, Binney & Tremaine 1987, Shlosman, Frank, & Begelman 1989, Athanassuola 1992a, 1992b, Phinney 1994), or the perturbations generated in an interaction with either a nearby neighbor (Toomre 1978; Dressel & Gallagher 1994), a merging event (Barnes & Hernquist 1991), or with an intergalactic medium (e.g., Kritsuk 1983).

3.4. *The Possible Origin of the String of Southwest* Hα *Knots*

3.4.1. *Is the String of Southwest* Hα *Emission Part of a Spiral Arm?*

The narrow-band images of NGC 3367 show emission from several sources tracing normal spiral arms. Would the southwest string of Hα sources be part of these normal spiral arms? The answer, as stated in § 2.2, is no. On one hand, an inspection of the Hα image shows that the spiral arms in the northwest part of the galaxy intersect the string at a considerable angle (ΔP.A. $\simeq 30°$). On the other hand, there seem to be two normal spiral arms on the southern region of the galaxy, but their emission peaks differ in distance by at least 10″, or about 2 kpc. That is, the normal spiral arm winds more tightly than the string of Hα sources labeled 1, 2, 3, 4, and 5 (see Fig. 5). Therefore, we conclude that the string is not part of any normal spiral arm.

3.4.2. *Is it Part of an OLR ring?*

Hα emission is a good tracer of star formation and, indirectly, it indicates the regions in which the gas densities have been increased by a certain mechanism. Barred galaxies, with nonaxisymmetric potentials, generally have regions with high gas densities at the so-called Lindblad resonances (Binney & Tremaine 1987).

The southwest string of Hα could be thought to be formed as a result of the dynamics imposed by the nonaxisymmetric bar potential, and it may be delineating the location of an outer resonance. Some barred galaxies show two rings that can be explained as forming at the Lindblad resonances: one at the inner Lindblad resonance (ILR), just around the compact nucleus, and another one at the outer Lindblad resonance (OLR), outside the stellar bar (for example, in NGC 1326; García-Barreto et al. 1991a; Buta 1995). The Lindblad resonances form at the radii at which $\Omega_p = \Omega_g \pm \kappa/m$, where Ω_p is the bar pattern speed, Ω_g is the angular velocity of the stellar disk, κ is the epicyclic frequency, and m is a positive integer. The minus sign corresponds to the ILR, and the plus sign corresponds to the OLR. Since there is no information on the velocity field of this galaxy, nor any estimation of Ω_p, we cannot determine the locations of the ILR or the OLR.

From the Hα data, as discussed before, there is no evidence for a circumnuclear ring unless it is smaller than ~ 200 pc in radius. Nonetheless, if the ILR exists, it should be located inside a galactocentric radius of about 200 pc. Thus, if we assume that NGC 3367 has a rotation curve (i.e., epicyclic frequencies) similar to those observed in late-type spirals then, for a slow bar pattern speed, the OLR should be at a radius of at least 10 kpc (Contopoulos & Grösbel 1989). Even though highly speculative, this is marginally consistent with the observed location of the southwest Hα string. Thus, at the moment it cannot be completely ruled out that the southwest string of Hα does belong to an OLR, but the fact that it is only evident as a semicircle of bright spots argues against this interpretation. The nondetection of a northeast semicircle could be the result of obscuration, but this would need additional (and very restrictive) assumptions about the galaxy inclination and the dust spatial distribution, both of which are not supported by observations (see Figs. 2 and 3). Another argument against an OLR interpretation is based in the statistical study done by Elmegreen et al. (1992), which suggests that late-type barred galaxies have no outer rings, or pseudorings (also, their numerical simulations indicate that the rings, when present, are slightly oval and parallel to the bar, and that the outer rings can be destroyed by tidal interactions). Clearly, future Fabry-Perot studies of the kinematics of the Hα emission would be extremely useful in clarifying this issue.

3.4.3. *Is it Due to the Interaction of NGC 3367 with Intergalactic Gas?*

Another possible interpretation is that the southwest string of Hα emission is the result of the interaction of NGC 3367 with intergalactic gas (IGG), as it travels to the southwest direction. Two possible arguments in favor of this interpretation are (*a*) the morphology of the galaxy, as seen in optical photographs, is reminiscent of a bow shock (see POSS plate 976, and Sandage 1962) and (*b*) X-ray emission from the NGC 3367 region, with a flux $F_X \simeq 4.7 \times 10^{-13}$ ergs cm^{-2} s^{-1}, was detected with the *Einstein Observatory* (Gioia et al. 1990; Stocke et al. 1991; Fabbiano et al. 1992).

The interaction of a galaxy with diffuse hot intergalactic gas has been suggested usually as a gas stripping mechanism (e.g., Gunn & Gott 1972; Haynes, Giovanelli, & Chincarini 1984). Kritsuk (1983) has studied this dynamical interaction for different relative orientations of the galaxy and its direction of motion. Regardless of the orientation, however, Kritsuk concludes that the inner gas layers of the disk must be clearly perturbed. The bow shock morphology of NGC 3367 suggests that ram pressure could be disturbing the external layers as the galaxy is traveling into the southwest direction. However, NGC 3367 is a relatively isolated system (it can even be considered as a field galaxy)

and, in order for ram pressure to work, one needs to justify the existence of a hot IGG. In addition, the gas content of NGC 3367 can be considered normal, and there is no indication of stripping in the recent past (see below). Also, the available data do not show any indication for a perturbation in the rest of the gas layers of the disk.

With respect to the X-ray emission, the possibilities are also interesting, but the conclusion is again negative. The X-ray detection corresponds to a field of 144″ by 144″, which includes NGC 3367. Stocke et al., as stated before, report an offset between the X-ray emission centroid and the optical nucleus position of the galaxy (which they assume is the position of the VLA brightest radio continuum source). The X-ray emission is extended beyond the optical diameter of the galaxy, specifically in the southwest direction. Figure 7 of Fabbiano et al. shows the contours of the X-ray emission superimposed on POSS image NGC 3367, which we reproduce as Figure 7.

Comparing the X-ray emission from NGC 3367 with that observed in other barred spiral galaxies, the X-ray luminosity of NGC 3367 seems to be greater than normal. Giuricin et al. (1991) have concluded, from a statistical analysis, that there is no difference between the X-ray properties of barred versus unbarred galaxies, except in the ratio of X-ray to radio luminosities. This result, they think, is due in part to the increased radio emission in barred galaxies. The X-ray luminosity of NGC 3367, $L_X \simeq 9 \times 10^{40}$ ergs s^{-1}, is between 2 to 300 times the luminosity of other normal spiral galaxies (Fabbiano & Trinchieri 1987). For example, it is 11 times that of IC 342, about 6 times that of M83, and about 300 times that of NGC 5253. Also, the ratio of the X-ray to far-infrared luminosities in NGC 3367 is about 1.5 times that of the average of the 12 galaxies listed in Table 4, and 4 times that of IC 342. Similarly, the ratio of the X-ray to blue luminosities is about 3.3 times higher than the average of the 12 galaxies in Table 4, and about 16 times that of IC 342. Thus, aside from the offset in the southwest region, there seems to be an excess of X-ray emission, which could be due to an increase in star formation (and its associated supernova rate) or to an interaction with a hot surrounding medium.

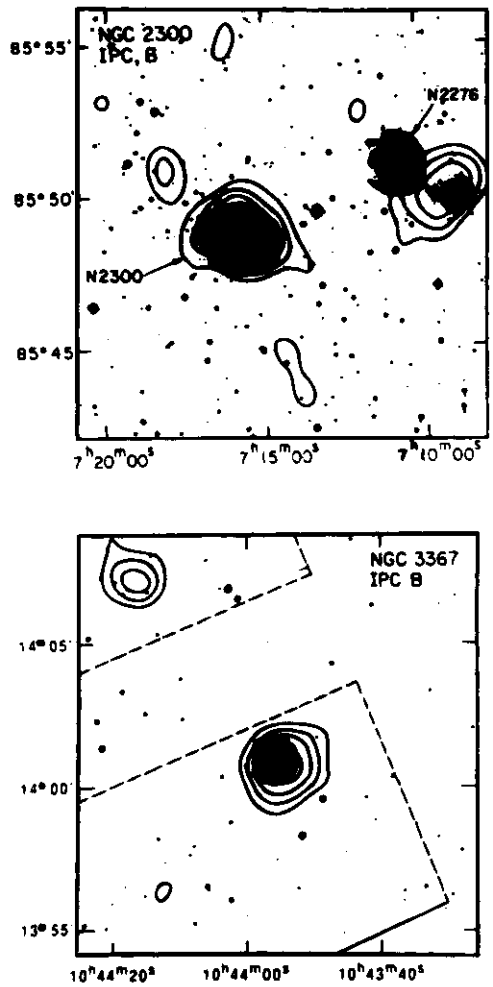

FIG. 7.—*Einstein* X-ray emission spatial distribution from the environment around NGC 2276 and NGC 3367; the optical images are POSS images (from Fabbiano et al. 1992).

If we assume that the excess is due to the interaction with the external gas, one finds a difficult problem. In general, a hot intergalactic gas (IGG) (with minimum temperatures of about $T \sim 10^7$ K) can be contained within the deep gravitational well from a group of galaxies (Sarazin 1986; Price et al. 1991). A galaxy with a similar string of Hα emission knots is NGC 2276 (see Fig. 7), in which the X-ray emission suggest an interaction with intergalactic gas (from the compact group of galaxies known as the NGC 2300 group). In contrast, NGC 3367 is a relatively isolated system without signs of a present tidal interaction with an external medium. Therefore, we disregard the possibility of an interaction with a hot medium. The excess in the X-ray emission then is likely due to an enhancement of star formation along the southwest string. New higher resolution X-ray observations would be very useful to test this interpretation.

3.4.4. *Is it the Result of a Distant Tidal Interaction?*

The barred spiral NGC 2276, mentioned above, is part of the NGC 2300 group and has an optical southwest morphology similar to the one of NGC 3367 (i.e., like a bow shock). It has a bright sharp edge with many bright knots around it (Shakhbazyan 1973). The Hα velocity field in NGC 2276 (Gruendl et al. 1993) and the detection of X-ray emission from the NGC 2300 group (Fabbiano et al. 1992; Mulchaey et al. 1993), suggest the idea that the string of Hα regions could be the result of two processes: the interaction of NGC 2276 with a hot intracluster gas and a tidal interaction with the elliptical galaxy NGC 2300 (Gruendl et al. 1993).

Figure 7 reproduces the X-ray distribution from the regions around NGC 2276 and NGC 3367 (from Fabbiano et al. 1992). There is a clear difference in these two objects: in NGC 3367 the emission peaks (with the offset described before) at the location of the galaxy, but in NGC 2276 the emission peaks in the region of the possible interaction (or where the IGG is either denser or hotter). The possibility of a tidal interaction is clear in the case of NGC 2276 since NGC 2300, an elliptical galaxy, is nearby. This is not the case in NGC 3367. The closest neighbor of NGC 3367 is also an elliptical galaxy, NGC 3419, but it is ~900 kpc away to the northeast direction (Tully 1988). A possibility that NGC 3367 could have had a tidal interaction with NGC 3419 is extremely low, since the time of interaction and lifetime of the southwest Hα string would not agree. So we disregard this possibility.

With respect to the possible interaction in NGC 2276, one can set some limits to the expected outcome. As in the case of NGC 3367, NGC 2276 is not H I deficient (it has H I Def ≃ 0.22), and there are no clear differences in the gaseous

TABLE 4

COMPARISON LIST OF ISOLATED GALAXIES WITH X-RAY EMISSION

Galaxy (NGC)	Type	D (Mpc)	L_X[a] (10^{39} ergs s^{-1})	L_B/L_{FIR}	L_X/L_B (10^{-5})	L_X/L_{FIR} (10^{-4})	SFR ($M_\odot$ yr^{-1})
628	Sc(s)	9.7	4.4	4.73	5.5	2.6	1.87
1313	SBc(s)	3.7	2.8	4.21	17.5	7.4	0.38
1559	SBc(s)	14.3	23.0	1.78	34.8	6.2	2.0
1672	Sb(rs)	14.5	17.0	1.02	33.3	3.4	1.95
2403	Sc(s)	4.2	4.0	5.87	9.1	5.3	0.99
2903	Sc(s)	6.3	6.4	2.83	12.5	3.5	1.33
4631	Sc	6.9	10.0	2.20	15.1	3.3	1.85
5236 (M83)	SBc	4.7	15.0	1.82	18.7	3.4	2.40
5253	Am	3.2	0.3	1.59	10.7	1.7	0.08
6744	Sbc(r)	10.4	9.0	100.0	4.2	42.8	4.10
6946	Sc(s)	5.5	11.0	3.87	9.1	3.5	2.92
IC342	Sc	3.9	7.9	8.30	3.1	2.6	5.4
Mean values[b]	...	...	...	3.47[c]	14.5	7.1	2.1
2276	S	36.8	41.0	1.50	22.7	3.4	5.80
2300	E	31.0	20000	...[d]	16129	...[d]	2.4
3367	SBc(s)	43.6	89.0	2.26	48.6	10.9	5.11

[a] X-ray luminosities from Fabbiano & Trinchieri 1987.
[b] Average of 12 galaxies (i.e., excluding NGC 2276, 2300, and 3367).
[c] Value excluding NGC 6744. With that galaxy, the value is 11.5.
[d] Not applicable since there are no FIR observations.

content of these two galaxies. Then there is no evidence for any recent gas removal. One can see that the IGG ram pressure is not able to strip the gas from the disk

$$P_{\rm ram} = \rho_{\rm igg} v_{\rm rel}^2 ,$$

where $\rho_{\rm igg} = n_{\rm igg} m_{\rm H}$ is the IGG volume mass density, $v_{\rm rel}$ is the relative velocity of the galaxy and the IGG, and $m_{\rm H}$ is the mass of a hydrogen atom. The pressure in the disk is given by the weight of the gas column density at midplane (e.g., Franco 1992)

$$P_{\rm grav} = \frac{\pi G \sigma_{\rm g} \sigma_t}{2} ,$$

where G is the gravitational constant, σ_g is the gas mass surface density, and $\sigma_t = \sigma_g + \sigma_*$ is the total mass surface density (if dark matter is included in the total mass, then, one has to estimate its contribution to the disk surface mass density). For the case of the IGG in the neighborhood of NGC 2276, one can use $n_{\rm igg} \sim 5 \times 10^{-4}$ cm^{-3} (Mulchaey et al. 1993). A lower limit for the disk pressure can be approximated with the H I surface gas density at a galactocentric distance of 10 kpc, $\sigma_g \geq 7 \times 10^{-4}$ g cm^{-2}, and from the blue luminosity, which traces part of the surface star density, $\sigma_* \geq 9 \times 10^{-3}$ g cm^{-2} (Gruendl et al. 1993). These values give the lower limit $P_{\rm grav} \simeq 8 \times 10^{-13}$. Thus, for $v_{\rm rel} \leq 300$ km s^{-1}, $P_{\rm ram} \leq P_{\rm grav}$, and the interaction with the hot gas could be only driving a shock inside the disk, without removing the perturbed gas. This implies that there is really *no* bow shock, because the shocked gas does not flow around the object, but it is likely that the string in NGC could be due (at least in part) to this interaction. Such a scenario cannot be applied to NGC 3367 because, as we have stated already, there is no evidence of intergalactic hot gas to interact with.

3.5. *An Off-Center Impact With an External Perturber: Gas Inflow to the Nucleus and the Formation of the Southwest String of* Hα *Sources*

As discussed by Lynds & Toomre (1976) and Toomre (1978), an off-center interaction of a disk galaxy with an intruder with a mass of $m_p \sim m_{\rm gal}/2$ creates crowding of stellar orbits in the disk galaxy. This produces a ringlike density wave that propagates outward from the point of collision. Such a wave should trigger, as a spiral arm does, star formation in those locations in which the gas can be collected into large cloud complexes. If the southwest string was created by such a process, then it can be envisioned as the present stage of an expanding ring of Hα-emitting regions. The possibility of observing any of the H II regions triggered by the wave in the past is obviously restricted by the average lifetime of photoionized regions. Given that massive stars cannot live longer than about 10^7 yr, and that expanding H II regions can destroy their parent clouds in even shorter timescales, the observability of the bright Hα knots is probably restricted to a few times 10^6 yr. Thus, with the Hα line one can only trace the most recent star formation episodes triggered by the expanding wave (i.e., one may trace a ring, at about a constant galactocentric radius, with the present location of newly born stars and their associated photoionized gas).

Collisions passing through the galaxy center would create circular star-forming structures, as in the case of the Cartwheel galaxy (e.g., Mihos & Hernquist 1994b; Gerber, Lamb, & Balsara 1996). Off-center collisions, however, would create elongated structures (Gerber & Lamb 1994). Large mass perturbers simply pass through the target galaxies and produce large wave amplitudes, with spectacular effects. Smaller intruders can also create bursts of star formation, but the resulting effects are modest, and the final fate of the intruders is less bright: they can be either swallowed by the target galaxy or destroyed during the interaction (see the merger model with a small satellite companion by Mihos & Hernquist 1994a). In the case of NGC 3367, one can imagine that the semicircle string was formed as a result of an off-center impact with a small companion. Given the present position of the half-ring and the expected wave velocity in the external parts of the disk (somewhat below $\sim$100 km s^{-1}; Salo, García-Barreto, & Franco 1996), the collision probably occurred some 10^8 yr ago. The expected lifetime of the expanding ring is difficult

to derive but, given that the wave amplitude depends on the strength of the collision (Lynds & Toomre 1976; Toomre 1978), it cannot be much longer than $\sim 10^8$ yr. Thus, the present string could well be delineating the final effects of the wave. This same process could also explain the relative misalignment between the normal arms and the southwest structure.

The fact that no large optical companion is presently near NGC 3367 is consistent with the idea that the intruder must have been compact (probably with very little gas for the interpenetration to be so clean). The perturbation of the impact can also induce internal torques in the gaseous disk and drive gas to the central regions of the galaxy. Similarly, if the intruder is swallowed by the galaxy, the process would also drive a gas inflow to the central regions. Thus, in this scenario, it is very likely that a rapid gas inflow has occurred and is now observed as ionized gas in the compact nucleus. Thus, the scheme is very appealing because one can explain simultaneously the presence of the string and the strong emission from the nucleus. There are two points of caution in this interpretation, however. First, one does not see any large optical companion to NGC 3367, and we interpreted this as evidence for a collision with a small intruder. Models with off-center collisions of a disk galaxy with small companion have been done by Gerber & Lamb (1994) and of a barred galaxy with small companions have been performed recently by Salo et al. The numerical experiments suggest that this scenario produces the required wave amplitude and observed shapes. Second, NGC 3367 has a well-ordered stellar bar which, as the experiments show, is not destroyed by the impact.

4. CONCLUSIONS

We have observed the barred galaxy NGC 3367 in the broadband *R* and *I* filters and in the narrow-band Hα filter. The Hα line is detected in the compact nucleus and in several places of the disk. Our main results are as follows:

1. The strongest Hα+N [II] emission is originated from the nucleus;
2. There is no Hα+N [II] emission detected from the stellar bar region;
3. The southwest region of the optical broadband images of the galaxy shows a sharp edge, similar to a bow shock, with no counterpart in the northeast side;
4. The Hα+N [II] regions in the southwest string lie at an average distance of 9–10 kpc from the nucleus, forming an almost 180° symmetrical structure (from the southeast to the northwest), being definitely not part of any normal spiral arm;
5. To understand the origin of this string of Hα emission knots, we have discussed several possible scenarios. We suggest that the origin of the southwest structure could be due to an interpenetration of NGC 3367 by an intruder at an off-center position, to the southwest, similar to the explanation suggested for ring galaxies by Lynds & Toomre (1976) and Toomre (1978). This scenario can also explain, due to the resulting gas inflow, the presence of gas in the nucleus.

The authors thank an anonymous referee for helpful comments and suggestions on how to improve the paper.

It is a pleasure to thank Alar Toomre and Heikki Salo for useful suggestions and discussions. We thank also M. Peimbert and E. Vásquez for a careful reading of the manuscript. We would like to acknowledge L. A. Martinez for assistance with the local IRAF version, and A. Garcia and Juan C. Yustis for the art and photographic work. J. A. G-B. acknowledges partial financial support from CONACYT (Mexico) grant 689-E9111. J. E. acknowledges the support given to this project by DGAPA-UNAM grant IN105894, CONACyT grant 400354-4843E, and an R&D Cray research grant.

REFERENCES

Athanassoula, E. 1992a, MNRAS, 259, 328
———. 1992b, MNRAS, 259, 345
Barnes, J. E., & Hernquist, L. E. 1991, ApJ, 370, L65
Binney, J., & Tremaine, S. 1987, Galactic Dynamics (Princeton: Princeton Univ. Press)
Buta, R. 1995, ApJS, 96, 39
Condon, J. J., Helou, G., Sanders, D. B., & Soifer, B. T. 1990, ApJS, 73, 359
Contopoulos, G., & Grösbol, P. 1989, A&A Rev., 1, 261
Dressel, L. L., & Condon, J. J. 1976, ApJS, 31, 187
Dressel, L. L., & Gallagher, J. S. III, 1994, in Mass-Induced Activity in Galaxies, ed. I. Shlosman (Cambridge: Cambridge Univ. Press), 165
Elmegreen, D. M., Elmegreen, B. G., Combes, F., & Bellin, A. D. 1992, A&A, 257, 17
Fabbiano, G., Kim, D.-W., & Trinchieri, G. 1992, ApJS, 80, 531
Fabbiano, G., & Trinchieri, G. 1987, ApJ, 315, 46
Franco, J. 1992, in Star Formation in Stellar Systems, ed. G. Tenorio-Tagle, M. Prieto, & F. Sanchez (Cambridge: Cambridge Univ. Press), 517
Gallouet, L., & Heidmann, N. 1971, A&AS, 3, 325
García-Barreto, J. A., Carrillo, R., Franco, J., Venegas, S., & Escalante-Ramirez, B. 1996, Rev. Mexicana Astron. Astrofis., in press
García-Barreto, J. A., Carrillo, R., Klein, U., & Dahlem, M. 1993, Rev. Mexicana Astron. Astrofis., 25, 31
García-Barreto, J. A., Dettmar, R.-J., Combes, F., Gerin, M., & Koribalski, B. 1991a, Rev. Mexicana Astron. Astrofis., 22, 197
García-Barreto, J. A., Downes, D., Combes, F., Gerin, M., Magri, C., Carrasco, L., & Cruz-Gonzalez, I. 1991b, A&A, 244, 257
Gerber, R. A., & Lamb, S. A. 1994, ApJ, 431, 604
Gerber, R. A., Lamb, S. A., & Balsara, D. S. 1996, MNRAS, 278, 345
Gioia, I. M., Maccacaro, T., Schild, R. E., Wolter, A., Stocke, J. T., Morris, S. L., & Henry, J. P. 1990, ApJS, 72, 567
Giovanardi, C., Helou, G., Salpeter, E. E., & Krumm, N. 1983, ApJ, 267, 35
Giovanelli, R., Chincarini, G. L., & Haynes, M. P. 1981, ApJ, 247, 383
Giuricin, G., Bertotti, G., Mardirossian, F., & Mezzetti, M. 1991, MNRAS, 250, 392
Grösbol, P. J. 1985, A&AS, 60, 261
Gruendl, R. A., Vogel, S. N., Davis, D. S., & Mulchaey, J. S. 1993, ApJ, 413, L81
Gunn, J. E., & Gott, R. J. 1972, ApJ, 176, 1
Haynes, M. P., Giovanelli, R., & Chincarini, G. L. 1984, ARA&A, 22, 445
Ho, L. C., Filippenko, A. V., & Sargent, W. L. W. 1995, ApJS, 98, 477
Huchtmeier, W. K., & Seiradakis, J. H. 1985, A&A, 143, 216
Humason, M. L., Mayall, N. U., & Sandage, A. R. 1956, AJ, 61, 97
IRAS Catalogs and Atlases: Volume 3, The Point Source Catalog. 1988 (Washington, DC: US Government Printing Office)
Kritsuk, A. G. 1983, Astrofizika, 19, 263
Lynden-Bell, D., & Kalnajs, A. J. 1972, MNRAS, 157, 1
Lynds, R., & Toomre, A. 1976, ApJ, 209, 382
Mihos, J. C., & Hernquist, L. 1994a, ApJ, 425, L13
———. 1994b, ApJ, 437, 611
Mirabel, I. F., & Sanders, D. B. 1988, ApJ, 335, 104
Mulchaey, J. S., Davis, D. S., Mushotzky, R. F., & Burstein, D. 1993, ApJ, 404, L9
Oke, J. B. 1974, ApJS, 27, 21
Oke, J. B., & Schild, R. E. 1970, ApJ, 161, 1015
Phinney, E. S. 1994, in Mass-Transfer Induced Activity in Galaxies, ed. I. Shlosman (Cambridge: Cambridge Univ. Press), 1
Price, R., Burns, J. O., Duric, N., & Newberry, M. V. 1991, AJ, 102, 14
Salo, H., Garcia-Barreto, J. A., & Franco, J. 1996, in preparation
Sandage, A. 1962, The Hubble Atlas of Galaxies (Washington, DC: Carnegie Inst. of Washington)
Sandage, A., & Tammann, G. A. 1981, A Revised Shapley-Ames Catalog of Bright Galaxies (Washington DC: Carnegie Inst. of Washington)
Sarazin, C. L. 1986, Rev. Mod. Phys., 58, 1
Scoville, N. Z., & Young, J. S. 1983, ApJ, 265, 148
Shakhbazyan, R. K. 1973, Astrophysics, 9, 9

Shlosman, I., Frank, J., & Begelman, M. C. 1989, Nature, 338, 45
Simkin, S. M., Su, H. J., & Schwarz, M. P. 1980, ApJ, 237, 404
Soifer, B. T., Boehmer, L., Neugebauer, G., & Sanders, D. B. 1989, AJ, 98, 766
Staveley-Smith, L., & Davies, R. D. 1988, MNRAS, 231, 833
Stocke, J. T., et al. 1991, ApJS, 76, 813
Telesco, C. M., Dressel, L. L., & Wolstencroft, R. D. 1993, ApJ, 414, 120
Toomre, A. 1978 in The Large Scale Structure of the Universe, ed. M. S. Longair & J. Einasto (Dordrecht: Reidel), 109
Tully, R. B. 1988, Nearby Galaxy Catalog (Cambridge: Cambridge Univ. Press)
Véron-Cetty, M.-P., & Véron, P. 1986, A&AS, 66, 335
Young, J. S., Schloerb, F. P., Kenney, J. D., & Lord, S. D. 1986, ApJ, 304, 443

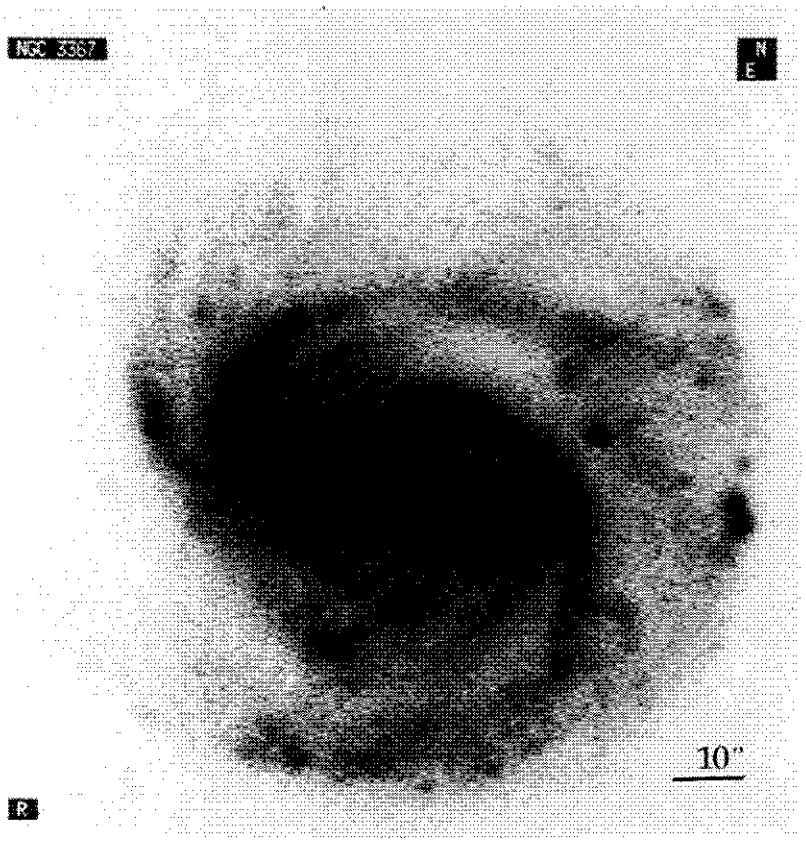

FIG. 1*a*

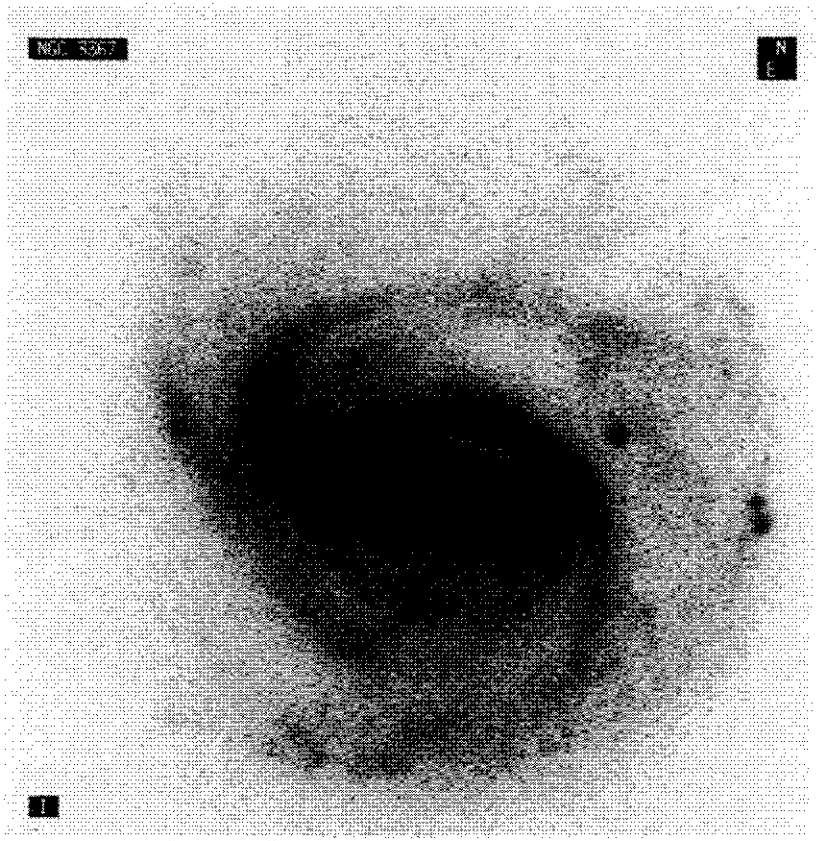

FIG. 1*b*

FIG. 1.—(*a*) Images of NGC 3367 in the broadband filter R ($\lambda_{central} \simeq 6340$ Å) in gray scale (*left*). The bar corresponds to an angular scale of 10″. The figures have not been amplitude calibrated. North is up, East is left. (*b*) Images in the broadband filter I ($\lambda_{central} \simeq 8040$ Å) in gray scale (*right*). Scale and orientation are the same as in (*a*).

GARCÍA-BARRETO, FRANCO, & CARRILLO (see 469, 139)

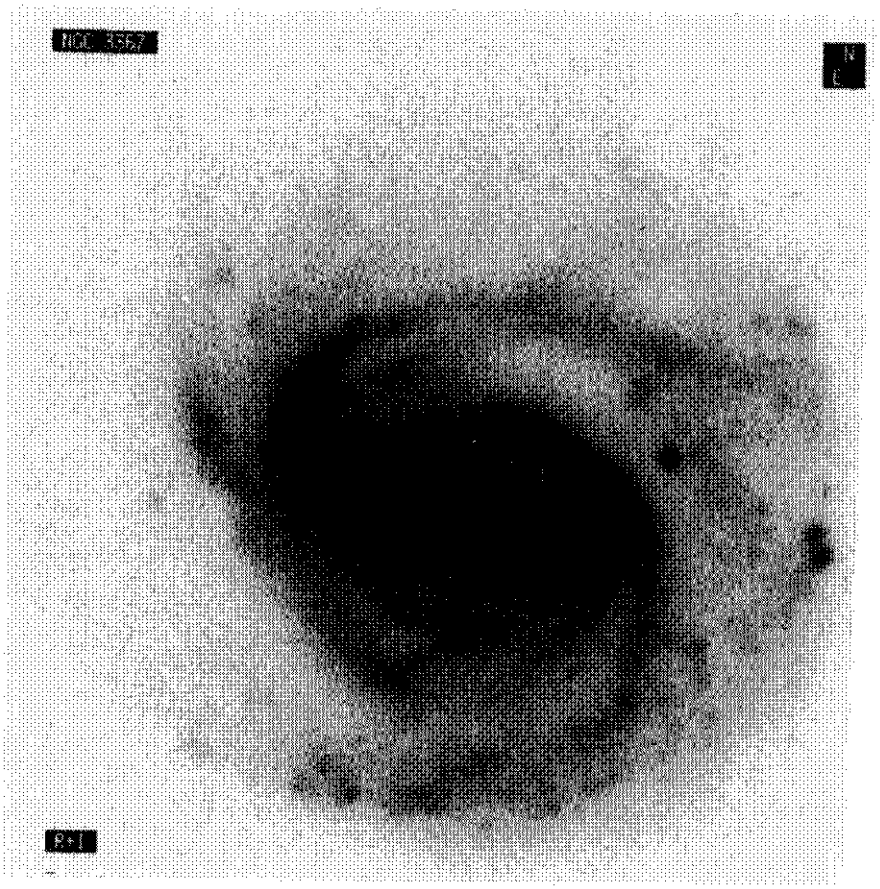

FIG. 2.—Image of the red continuum, $R+I$, of NGC 3367. Scale and orientation are the same as in Fig. 1*a*.

GARCÍA-BARRETO, FRANCO, & CARRILLO (see 469, 139)

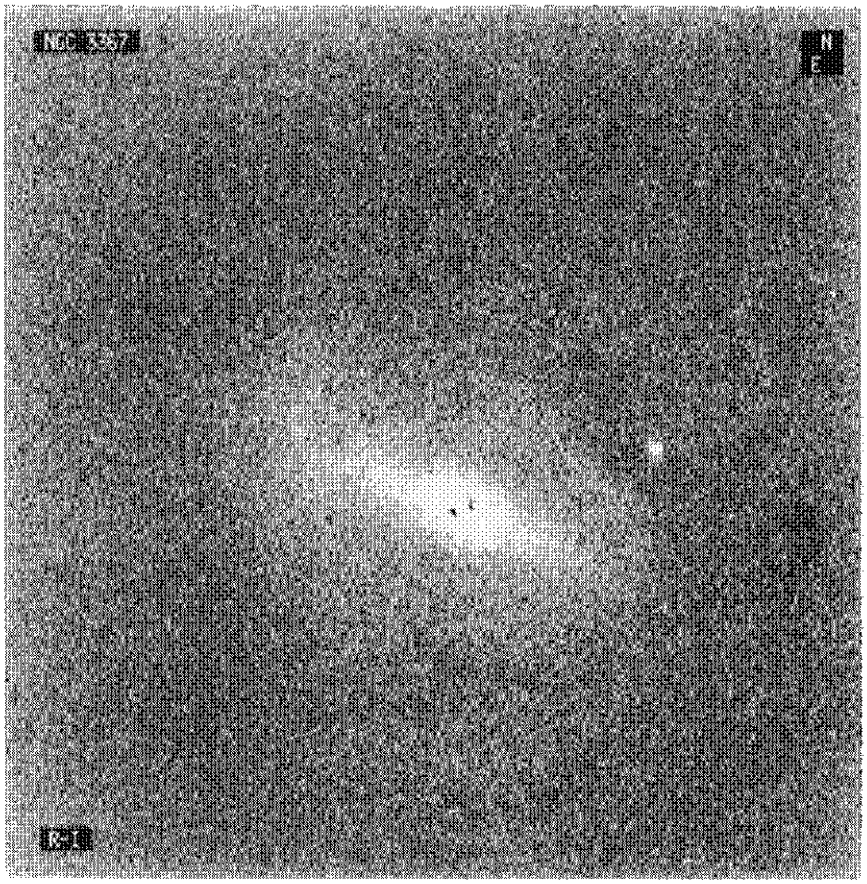

FIG. 3.—Image of the color index $R-I$ of NGC 3367. Notice that there is no sign of obvious extinction either in the northeast or the east side of the galaxy. Scale and orientation are the same as in Fig. 1*a*.

GARCÍA-BARRETO, FRANCO, & CARRILLO (see 469, 139)

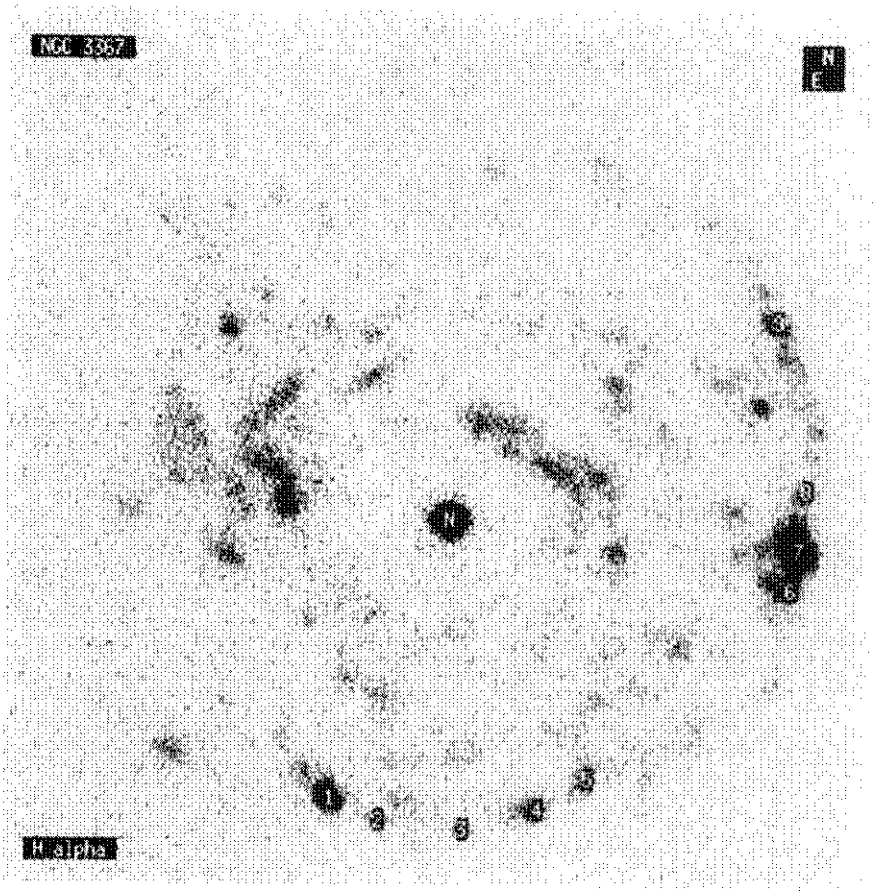

FIG. 4.—Images of NGC 3367 in the narrow-band filter Hα (after substraction of the continuum) in gray scale. Scale and orientation are the same as in Fig. 1. Gray scale is proportional to flux (see Table 2).

PLATE 6

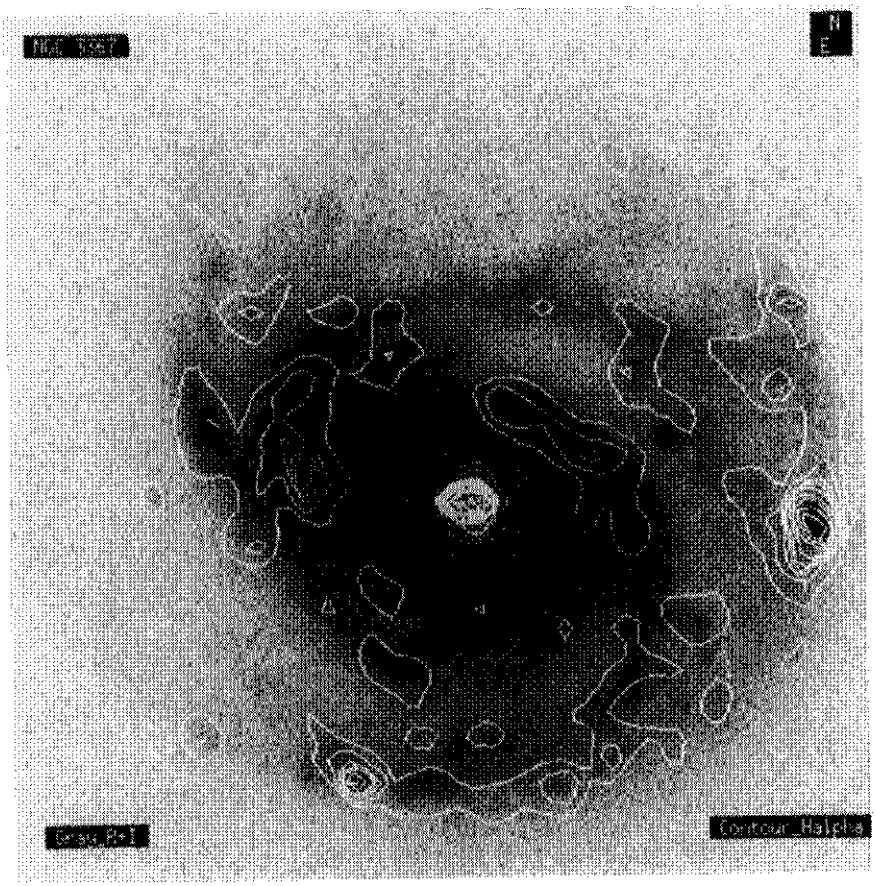

FIG. 5.—Image of the Hα emission, in contours, superimposed on a red continuum $R+I$ image (in gray). Scale and orientation are the same as in Fig. 1.